Ideal Two-Dimensional Electron Systems with a Giant Rashba-Type Spin Splitting in Real Materials: Surfaces of Bismuth Tellurohalides

S. V. Eremeev,[1,2,3] I. A. Nechaev,[2,3] Yu. M. Koroteev,[1,2,3] P. M. Echenique,[3,4,5] and E. V. Chulkov[3,4,5]

[1]*Institute of Strength Physics and Materials Science, 634021, Tomsk, Russia*
[2]*Tomsk State University, 634050, Tomsk, Russia*
[3]*Donostia International Physics Center (DIPC), 20018 San Sebastián/Donostia, Basque Country, Spain*
[4]*Departamento de Física de Materiales UPV/EHU, Facultad de Ciencias Químicas, UPV/EHU, Apdo. 1072, 20080 Sebastián/Donostia, Basque Country, Spain*
[5]*Centro de Física de Materiales CFM-MPC, Centro Mixto CSIC-UPV/EHU, 20080 San Sebastián/Donostia, Basque Country, Spain*

(Received 9 March 2012; published 13 June 2012)

Spintronics is aimed at actively controlling and manipulating the spin degrees of freedom in semiconductor devices. A promising way to achieve this goal is to make use of the tunable Rashba effect that relies on the spin-orbit interaction in a two-dimensional electron system immersed in an inversion-asymmetric environment. The spin-orbit-induced spin splitting of the two-dimensional electron state provides a basis for many theoretically proposed spintronic devices. However, the lack of semiconductors with large Rashba effect hinders realization of these devices in actual practice. Here we report on a giant Rashba-type spin splitting in two-dimensional electron systems that reside at tellurium-terminated surfaces of bismuth tellurohalides. Among these semiconductors, BiTeCl stands out for its isotropic metallic surface-state band with the $\bar{\Gamma}$-point energy lying deep inside the bulk band gap. The giant spin splitting of this band ensures a substantial spin asymmetry of the inelastic mean free path of quasiparticles with different spin orientations.

DOI: 10.1103/PhysRevLett.108.246802 PACS numbers: 73.20.−r, 71.70.Ej, 72.25.Dc

The spin-orbit interaction (SOI) that causes spin splitting of electron states in inversion-asymmetric systems [1–3] is expected to be efficiently exploited in spintronics. Even in the case of inversion-symmetric bulk materials, the spin splitting induced by the SOI appears in two-dimensional (2D) geometries, such as, e.g., metal surfaces [4–6], metallic surface alloys [7,8], and semiconductor heterostructures [9,10]. This Rashba effect leads to shifting of opposite spin-polarized bands by the momentum k_R in opposite directions. In semiconductor 2D electron systems, due to the Rashba effect there is a possibility for controllable spin manipulation via an applied electric field [11–13] that provides a pathway to the technological development and miniaturization of spintronics devices. The key operating characteristic here is the magnitude of the SOI-induced spin splitting characterized by the Rashba energy of split states E_R and the Rashba coupling parameter $\alpha_R = 2E_R/k_R$, which measures the strength of the spin splitting.

For the conventional narrow-gap semiconductor structures, the parameter α_R is of order of 10^{-1} eV Å [13]. Such a small α_R hampers the development of spintronics devices for room-temperature applications since the latter require a significantly greater spin splitting. Recently found systems that demonstrate a large spin splitting of 2D-electron states (α_R is about 1 order of magnitude greater than that in the semiconductor 2D systems) are noble-metal-based Bi-surface alloys [8,14–16]. However, in this case metallic substrates prevent tuning the spin splitting by external electric field and making a surface spin signal detectable because of the large bulk current.

Apart from spintronics applications, the large Rashba splitting is strongly desired also for a semiconductor film that being sandwiched between an *s*-wave superconductor and a magnetic insulator can be used in a setup for creating and manipulating Majorana fermions for topological quantum computation [17]. To advance in the search for a semiconductor 2D system with large and tunable spin splitting, we consider such a class of layered semiconductors as bismuth tellurohalides. Interest in these materials has been triggered by recently published results [18–20], which have revealed a giant Rashba-type spin splitting of bulk states in BiTeI.

In the present Letter, we examine two 2D geometries of bismuth tellurohalide compounds: Te- and haloid-terminated surfaces. On the basis of *ab initio* calculations, we show that the 2D electron systems are formed at the Te-terminated surface of bismuth tellurohalides in electron surface states (SSs), which split off from the bulk conduction band and, hence, inherit the giant spin splitting and spin structure from the bulk states. These spin-split SSs provide unique quasiparticle properties of the respective 2D systems, which we analyze within the G^0W^0 approximation. We show that among the considered bismuth tellurohalides, the BiTeCl compound should be an ideal candidate for a very promising material for spintronics applications.

The bismuth tellurohalides BiTeCl, BiTeBr, and BiTeI have hexagonal crystal structures [21] (see Fig. 1). BiTeI is

 © 2012 American Physical Society

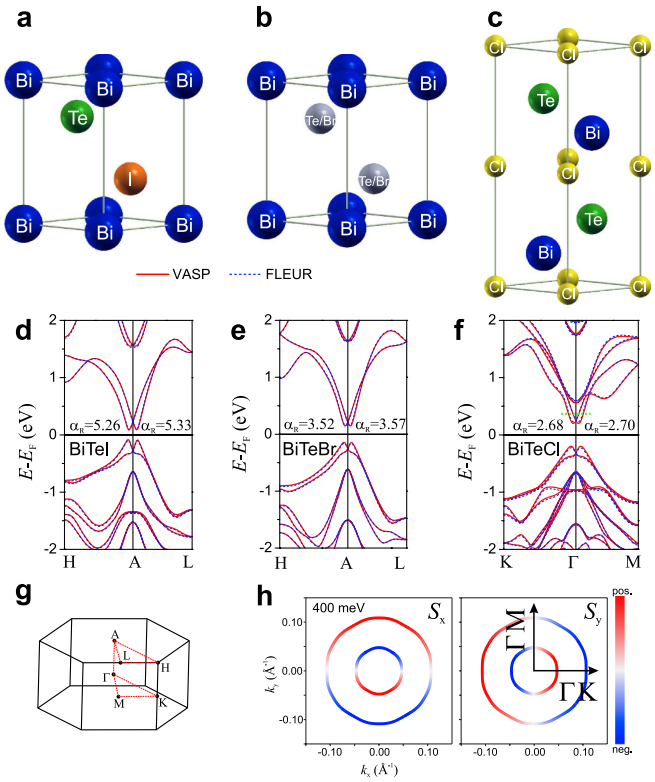

FIG. 1 (color online). Atomic crystal structure (a)–(c) and bulk band spectra of BiTe X ($X = I$, Br, Cl) compounds (d)–(f) calculated by the VASP (solid lines) and FLEUR codes (dashed lines) along high symmetry directions of the Brillouin zone. Band structure for BiTeBr calculated for BiTeI-type ordered phase. Values of α_R for conduction bands in the AH and AL (ΓK and ΓM for chloride) directions are shown. Brillouin zone of the hexagonal cell (g). Spin-resolved constant energy contours for conduction band states in BiTeCl at 400 meV (h).

composed by Bi, Te, and I layers stacking along the c axis. The structure of BiTeBr differs from that of BiTeI by tellurium and bromine atoms randomly distributed within the Te and Br atomic layers. In BiTeCl, the tellurium and chlorine layers alternate along the c direction of the unit cell, forming a four-layered packing [21]. All these compounds are characterized by ionic bonding and pronounced three-layered (TL) structure, where the distance between TLs is about one and a half times greater than interlayer distances within the Te-Bi-X (X = Cl, Br, I) TL structure.

For structural optimization and electronic bands calculations, we employed density functional theory with the generalized gradient approximation (GGA) of Ref. [22] for the exchange-correlation (XC) potential within the projector augmented wave method as implemented in VASP [23,24]. Complementary calculations of bulk electronic bands were performed using the full-potential linearized augmented plane-wave (FLAPW) method as implemented in the FLEUR code [25] also within the GGA of Ref. [22] for the XC potential. The FLAPW basis has been extended by local orbitals (see Refs. [26,27]) to treat quite shallow semicore d states. Additionally, to reduce linearization error and accurately describe unoccupied states [28], we have included for each atom one local orbital per angular momentum up to $l = 3$.

In Fig. 1, we show the bulk band structures calculated by VASP and FLEUR codes for the considered bismuth tellurohalides. As seen in the figure, VASP gives almost the same band structures as FLEUR. In the case of BiTeI, the obtained electronic bands are in good agreement with earlier WIEN-code calculations [19]: both the conduction-band minimum (CBM) and the valence-band maximum (VBM) demonstrate giant Rashba-type spin splitting with $k_R \approx 0.055$ Å^{-1} in the vicinity of the A point. However, our calculated α_R is larger than that obtained in Ref. [19] that can mainly be attributed to larger E_R. It is worth noting that the FLEUR calculations performed without recourse to linearization error corrections give $\alpha_R \approx 4.8$ eV Å that is close to $\alpha_R \approx 4.5$ eV Å found in Ref. [19].

In BiTeBr, the Rashba-type splitting of bulk CBM and VBM bands decreases along with the increase of the band gap. In BiTeCl, the folding of the Brillouin zone along the k_z direction leads to transfer of the band gap to the Γ point. As one can see, the lighter X atom leads to widening of the band gap and to reduction of α_R. Note that the $\Gamma K/\Gamma M$ anisotropy of spin splitting in BiTeCl is the lowest one among the considered compounds. The spin-resolved constant energy contours (CEC) for BiTeCl [Fig. 1(h)] demonstrate almost perfect circular shape for both inner and outer branches of the Rashba-split conduction band. This feature is distinct from the calculated CEC for BiTeI in Ref. [18], which shows a hexagonal shape for the outer branch. This deviation of CEC from the circular shape is accompanied by sizeable out-of-plane spin component S_z in BiTeI [18], whereas in BiTeCl the Rashba-split state has S_z close to zero (not shown).

The surface of BiTeCl and BiTeI formed under cleavage between neighboring TL can have two possible terminations: Te-layer termination or Cl(I)-layer termination, whereas in BiTeBr only the Te/Br mixed layer termination can be realized. We do not consider the latter surface in the present study.

For the VASP simulation of the semi-infinite BiTeCl(0001) with Te-terminated surface, we passivated the Cl termination of the 8 TL slab by a hydrogen monolayer. The electronic band spectrum of this slab is shown in Figs. 2(a) and 2(b). As is clearly seen, at the Te-terminated surface the spin-orbit split SS arises well below the conduction band and is spatially localized in the topmost TL. The state is mainly formed by orbitals of the surface Te and subsurface Bi atoms [Figs. 2(c) and 2(d)]. Within the energy gap region, the energy dispersion of the SS demonstrates the free-electron-like parabolic character. The spin splitting of the state in the $\bar{\Gamma}$-$\bar{M}$ direction is characterized by $\alpha_R = 1.78$ eV Å.

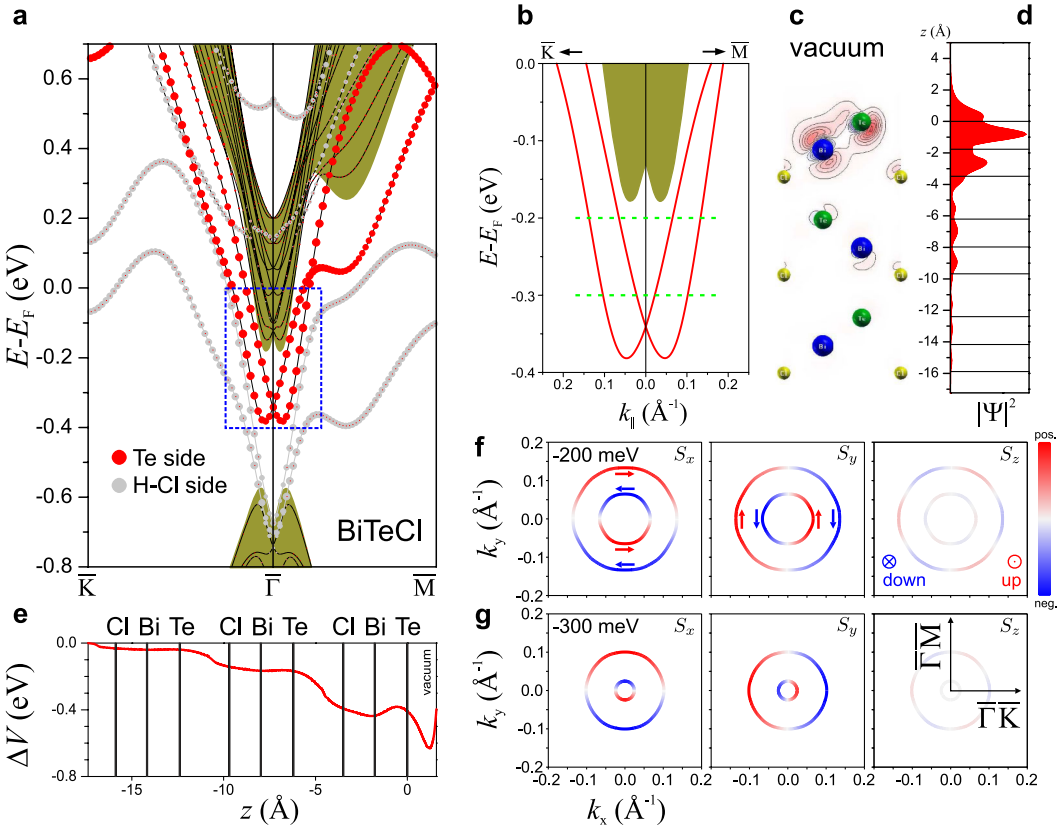

FIG. 2 (color online). (a) Band structure of an 8-TL thick BiTeCl(0001) slab with hydrogen on Cl-terminated side; the red (dark gray) and light gray bands are states from the Te- and H-terminated side of the slab, respectively. The size of the red (dark gray) and light gray circles denotes weights of the states localized in opposite, Te and H-Cl terminations of the slab, respectively. The projected bulk band structure is shown in olive green (shaded area). (b) A magnified view of electronic structure of Te-terminated BiTeCl(0001) surface in the vicinity of $\bar{\Gamma}$ [$E(k_{\parallel})$ ranges correspond to dashed frame marked in the panel (a)]. Spatial distribution of the Rashba-split state charge density in the $(11\bar{2}0)$ plane (c) and integrated over (x, y) planes (d). The change of the potential in near-surface layers of the crystal with respect to that in central, bulklike layers (e). Spin structure of the Rashba-split states on Te-terminated BiTeCl(0001), as given by spin projections S_x, S_y, and S_z at energies of -200 meV (f) and -300 meV (g).

The spin-resolved CEC for the Rashba-split SSs on Te-terminated BiTeCl(0001) at -200 and -300 meV demonstrate circular shape in the gap region with the spin polarization inherited from the bulk conduction band. Similar to the states in the bulk conduction band, the SS is almost completely in-plane spin-polarized but the S_z spin component increases slightly when approaching the conduction-band bottom.

The emergence of the SS can be understood from analysis of changes of the near-surface potential. In Fig. 2(e) this change marked as ΔV is shown. Owing to the pronounced TL structure, the observed ΔV is stepwise. Trapping of electrons of the outermost TL in the surface potential well splits off the Rashba SS from the bulk conduction band and noticeably increases its effective mass. Additionally, the presented ΔV reflects modifications of the potential within the outermost TL, which lead to decreasing the strength α_R with the unchanged atomic contribution to the latter.

To complete the picture of surface properties of BiTeCl, we examine its Cl-terminated surface. As in the previous case it is simulated by the 8 TL slab with hydrogen on the opposite (Te-terminated) side of the slab. In contrast to the Te-terminated surface, on the Cl-terminated BiTeCl(0001) surface the positive ΔV (which is 2 times larger by magnitude than that on the Te-terminated surface; see Fig. S1(a) of Supplemental Material [29]) splits off the valence-band edge states, forming in the gap a pair of spin-split SSs with negative effective masses (Fig. S1(b) of Supplemental Material [29]). Owing to noticeable anisotropy of the SS dispersion of the upper state, the CEC shown in Fig. S1(c) has more complex shape. Another feature of the SSs on Cl-terminated surface is that they are appreciably out-plane spin polarized. Because of above-mentioned features and the fact that under the degeneracy point the branches of the spin-split states are practically in immediate proximity to each other, this Cl-terminated surface has less appeal than the Te-terminated one.

Apparently, the revealed electronic structure of the Te-terminated surface of BiTeCl represents a unique case that combines the giant spin splitting characteristic of

noble-metal-based Bi-surface alloys and the controllability of semiconductor low-dimensional systems. Various chemical and physical phenomena at such a surface may be determined by decay of elementary excitations on the surface. In order to gain insight into quasiparticle dynamics at the Te-terminated surface of BiTeCl, we consider here the inelastic decay caused by electron-electron scattering in the 2D electron system formed by electrons in the SS.

Because of the fact that the surface-state wave function is mostly confined within the topmost TL [see Fig. 2(d)] and that the $\bar{\Gamma}$-point energy of this SS lies deep inside the bulk band gap, we suppose that to a certain extent the respective 2D electron system can be an isolated one. As a consequence, the behavior of quasiparticles in such a system can be adequately described within the G^0W^0 scheme of Ref. [30] based on the Rashba model (respective material parameters, see in Sec. S2 of Supplemental Material [29]). By performing G^0W^0 calculations, we examine hole and electron excitations in the energy region that does not contain bulk-projected states.

The G^0W^0 results obtained with different values of the Fermi energy (E_F) in the mentioned 2D system are shown in Fig. 3. Since the chemical potential can be continuously tuned by doping or applied electric field, the considered locations of the Fermi level are realizable in practice. The results presented in Fig. 3 predict unique peculiarities for the considered 2D system. The first one is a noticeable difference between the inelastic decay rates $\Gamma_{\rm inner}$ and $\Gamma_{\rm outer}$, which is observed in the electron excitations energy region. This difference means that the inelastic decay rate depends on the branch of the spin-orbit split band and, as a consequence, on spin orientation for a given direction of $\mathbf{k}$. The ratio $\Gamma_{\rm outer}/\Gamma_{\rm inner}$ demonstrates dependence on energy, which varies strongly with E_F. The ratio reflects a spin asymmetry of the decay rate and, owing to equal quasiparticle velocities at a given energy for both branches, characterizes the ratio of the corresponding inelastic mean free paths (IMFP) of electrons carrying different spin. The resulting IMFP spin asymmetry is essentially bigger [especially in the cases shown in Figs. 3(c) and 3(d)] than that in 2D electron systems with small α_R values (see Ref. [31]) and amounts to values which are already well comparable with those in ferromagnets (see, e.g., Ref. [32]). However, as distinct from ferromagnetic materials, in our case the values of the IMFP spin asymmetry can be tuned by external electric field that modifies α_R.

As regards the mentioned spin asymmetry, the most interesting case is that shown in Fig. 3(d), where within the energy interval of ~60 meV the ratio, being measured from unity, changes its sign. This effect is caused by opening the plasmon decay channel for interbranch transitions with quite small momenta and finite energies. The same reason leads to the appearance of a "loop" in the energy dependence of $\Gamma_{\rm outer}$ in the hole excitations region below the degeneracy point E_0 [see Figs. 3(a) and 3(b)]. This is the second unique peculiarity of the considered 2D electron system, which can easily be resolved experimentally due to the revealed giant spin splitting of the SS (see Sec. S3 of the Supplemental Material [29]).

Now we turn to the Te-terminated surface of BiTeI. Such a surface also holds the Rashba-split SS (see Fig. S2(a) of Supplemental Material [29]) well reproducing the angle-resolved photoemission spectroscopy data [18]. The calculated $\alpha_R = 3.5$ eV Å is in good agreement with the value of 3.8 eV Å reported in Ref. [18]. In contrast to BiTeCl, the SS of BiTeI is less split off from the bulk conduction band

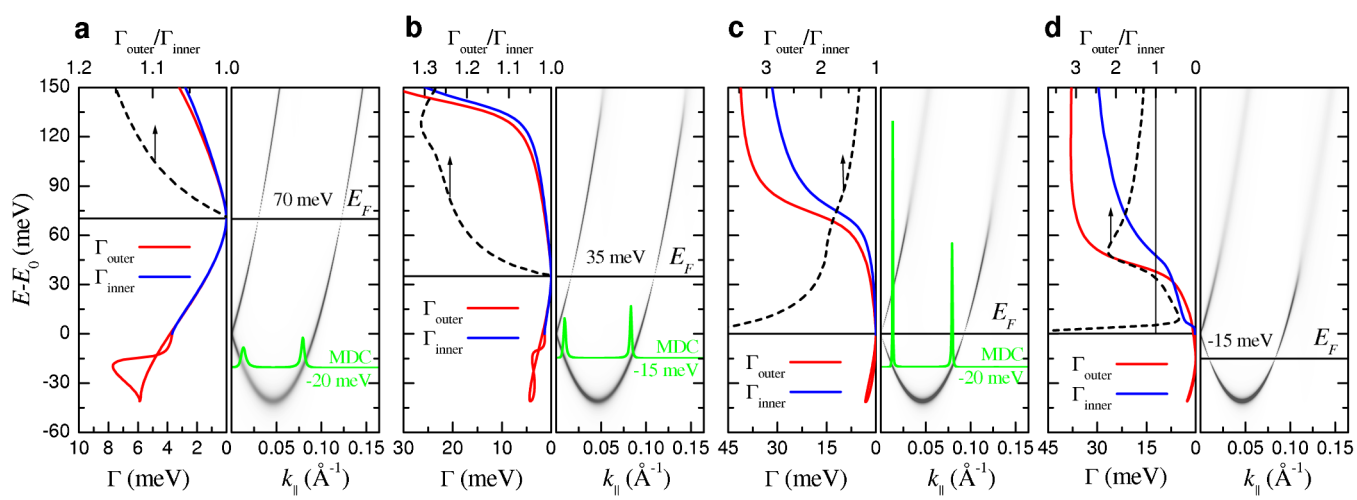

FIG. 3 (color online). Surface-state quasiparticle dynamics at the Te-terminated surface of BiTeCl. Left side of each panel: the inelastic decay rate for the inner and the outer branch ($\Gamma_{\rm inner}$ and $\Gamma_{\rm outer}$) and the ratio $\Gamma_{\rm outer}/\Gamma_{\rm inner}$ for electron excitations as functions of energy. Right side of each panel: contour plot of the respective quasiparticle spectral function and the momentum distributed curve (MDC) in arbitrary units and in the scale that is unified for all the panels presented (see Sec. S3 of Supplemental Material [29]). Energy is measured from the degeneracy point E_0. Values of the Fermi energy E_F as well as the energy at which the MDC has been calculated are indicated.

and penetrates deeper into subsurface TLs [Fig. S2(b)]. Below the conduction-band bottom the outer branch CEC has hexagonal shape [Fig. S2(c)], and thus it can not be precisely described by the isotropic Rashba model.

Thus, we have scrutinized the bulk and surface band structures of bismuth tellurohalides. We have shown that the giant spin splitting of the SSs is inherited from that of bulk states. The SSs emerge by splitting off from the bulk conduction (at Te-terminated surfaces) or valence (at haloid-terminated surfaces) bands owing to modifications in the potential within the near-surface layers. We have found that the 2D spin-orbit coupled electron system that can be formed by SS electrons hosted by the Te-terminated surface of BiTeCl possesses large spin asymmetry of the inelastic mean free path of electron excitations. We believe that our findings will stimulate further theoretical and experimental investigations of layered polar semiconductors as materials which meet the requirements for successful spintronics applications.

We acknowledge partial support by the University of the Basque Country (Project No. GV-UPV/EHU, Grant No. IT-366-07) and Ministerio de Ciencia e Inovación (Grant No. FIS2010-19609-C02-00). E. V. C. thanks J. Fabian for enjoyable discussions.

[1] E. I. Rashba, Sov. Phys. Solid State **2**, 1109 (1960); Y. A. Bychkov and E. I. Rashba, JETP Lett. **39**, 78 (1984); J. Phys. C **17**, 6039 (1984).
[2] G. Dresselhaus, Phys. Rev. **100**, 580 (1955).
[3] M. I. Dyakonov and V. Y. Kachorovskii, Sov. Phys. Semicond. **20**, 110 (1986).
[4] S. LaShell, B. A. McDougall, and E. Jensen, Phys. Rev. Lett. **77**, 3419 (1996).
[5] M. Hoesch, M. Muntwiler, V. N. Petrov, M. Hengsberger, L. Patthey, M. Shi, M. Falub, T. Greber, and J. Osterwalder, Phys. Rev. B **69**, 241401(R) (2004).
[6] Yu. M. Koroteev, G. Bihlmayer, J. E. Gayone, E. V. Chulkov, S. Blügel, P. M. Echenique, and Ph. Hofmann, Phys. Rev. Lett. **93**, 046403 (2004).
[7] T. Nakagawa, O. Ohgami, Y. Saito, H. Okuyama, M. Nishijima, and T. Aruga, Phys. Rev. B **75**, 155409 (2007).
[8] C. R. Ast, J. Henk, A. Ernst, L. Moreschini, M. C. Falub, D. Pacilé, P. Bruno, K. Kern, and M. Grioni, Phys. Rev. Lett. **98**, 186807 (2007).
[9] G. Lommer, F. Malcher, and U. Rossler, Phys. Rev. Lett. **60**, 728 (1988).
[10] J. Luo, H. Munekata, F. F. Fang, and P. J. Stiles, Phys. Rev. B **41**, 7685 (1990).
[11] M. Studer, G. Salis, K. Ensslin, D. C. Driscoll, and A. C. Gossard, Phys. Rev. Lett. **103**, 027201 (2009).
[12] S. Datta and B. Das, Appl. Phys. Lett. **56**, 665 (1990).
[13] J. Nitta, T. Akazaki, H. Takayanagi, and T. Enoki, Phys. Rev. Lett. **78**, 1335 (1997).
[14] G. Bihlmayer, S. Blugel, and E. V. Chulkov, Phys. Rev. B **75**, 195414 (2007).
[15] C. R. Ast *et al.*, Phys. Rev. B **77**, 081407(R) (2008).
[16] H. Mirhosseini, J. Henk, A. Ernst, S. Ostanin, C.-T. Chiang, P. Yu, A. Winkelmann, and J. Kirschner, Phys. Rev. B **79**, 245428 (2009).
[17] J. D. Sau, R. M. Lutchyn, S. Tewari, and S. DasSarma, Phys. Rev. Lett. **104**, 040502 (2010).
[18] K. Ishizaka *et al.*, Nature Mater. **10**, 521 (2011).
[19] M. S. Bahramy, R. Arita, and N. Nagaosa, Phys. Rev. B **84**, 041202(R) (2011).
[20] J. S. Lee, G. A. H. Schober, M. S. Bahramy, H. Murakawa, Y. Onose, R. Arita, N. Nagaosa, and Y. Tokura, Phys. Rev. Lett. **107**, 117401 (2011).
[21] A. V. Shevelkov, E. V. Dikarev, R. V. Shpanchenko, and B. A. Popovkin, J. Solid State Chem. **114**, 379 (1995).
[22] J. P. Perdew, K. Burke, and M. Ernzerhof, Phys. Rev. Lett. **77**, 3865 (1996).
[23] G. Kresse and J. Furthmüller, Comput. Mater. Sci. **6**, 15 (1996).
[24] G. Kresse and D. Joubert, Phys. Rev. B **59**, 1758 (1999).
[25] http://www.flapw.de.
[26] D. Singh, Phys. Rev. B **43**, 6388 (1991).
[27] E. Sjöstedt, L Nordström, and D. J Singh, Solid State Commun. **114**, 15 (2000).
[28] E. E. Krasovskii, Phys. Rev. B **56**, 12866 (1997).
[29] See Supplemental Material at http://link.aps.org/supplemental/10.1103/PhysRevLett.108.246802 for electronic structure of Cl-terminated BiTeCl and Te-terminated BiTeI surfaces, material parameters for the Rashba model, and details of the MDC calculations.
[30] I. A. Nechaev and E. V. Chulkov, Phys. Solid State **51**, 1772 (2009).
[31] I. A. Nechaev, P. M. Echenique, and E. V. Chulkov, Phys. Rev. B **81**, 195112 (2010).
[32] I. A. Nechaev and E. V. Chulkov, Eur. Phys. J. B **77**, 31 (2010).